

# Scanning Calorimetry and Fourier-Transform Infrared Studies into the Thermal Stability of Cleaved Bacteriorhodopsin Systems<sup>†</sup>

Ana I. Azuaga,<sup>‡</sup> Francesc Sepulcre,<sup>§</sup> Esteve Padrós,<sup>§</sup> and Pedro L. Mateo<sup>\*,‡</sup>

Departamento de Química Física, Facultad de Ciencias, e Instituto de Biotecnología, Universidad de Granada, 18071 Granada, Spain, and Unitat de Biofísica, Departament de Bioquímica i de Biologia Molecular, Facultat de Medicina, Universitat Autònoma de Barcelona, 08193 Bellaterra, Barcelona, Spain

Received July 24, 1996<sup>®</sup>

**ABSTRACT:** Differential scanning calorimetry and Fourier-transform infrared spectroscopy have been used to characterize the thermal stability of bacteriorhodopsin (BR) cleaved within different loops connecting the helical rods. The results are compared to those of the native protein. We show that the denaturation temperature and enthalpy of BR cleaved at peptide bond 71–72 or 155–156 are lower than those of the intact protein, and that these values become even lower for the BR cleaved at both peptide bonds. The effect of cleavage on the denaturation temperature and enthalpy values seems to be additive as has been previously suggested [Khan, T. W., Sturtevant, J. M., & Engelman, D. M. (1992) *Biochemistry* 31, 8829]. The thermal denaturation of all the samples was irreversible and scan-rate dependent. When cleaved at the 71–72 bond BR follows quantitatively the predictions of the two-state kinetic model at pH 9.5, with an activation energy of 374 kJ/mol, similar to that of native BR. Calorimetry experiments with different populations of intact and cleaved BR provide direct evidence for some intermolecular cooperativity upon denaturation. The denatured samples maintain a large proportion of  $\alpha$  helices and  $\beta$  structure, a fact which seems to be related to their low denaturation enthalpy as compared to that of water-soluble, globular proteins.

Thermodynamic-data analysis and energetic characterization of the thermal stability of membrane proteins (Sanchez-Ruiz & Mateo, 1987; Ruiz-Sanz et al., 1992) as well as that of several globular proteins (Sanchez-Ruiz et al., 1988; Conejero-Lara et al., 1991) cannot be undertaken because of their non-equilibrium, irreversible denaturation (Sanchez-Ruiz, 1992). This irreversibility is usually due to non-equilibrium processes taking place on protein unfolding (Klibanov & Ahern, 1987). Even in this case differential scanning calorimetry (DSC)<sup>1</sup> can provide the denaturation enthalpy ( $\Delta H$ ) and temperature ( $T_m$ ) values of the transition for a given scan rate. Thus  $T_m$  can be used as an operative parameter, at least in comparative, relative terms, to characterize the thermal stability of a protein which unfolds under non-equilibrium conditions. Fourier-transform infrared spectroscopy (FTIR) is a very suitable technique to complement protein DSC studies, particularly in the case of membrane proteins, since it provides structural information concerning the native and denatured states and can also be used to

observe the denaturation process itself (Surewicz & Mantsch, 1988; Surewicz et al., 1993; Arrondo et al., 1993; Jackson & Mantsch, 1995).

Bacteriorhodopsin (BR), the only protein present in the purple membrane of *Halobacterium salinarum*, is one of the best known and well-studied intrinsic membrane proteins, both from a structural and a functional point of view (Henderson et al., 1990; Rothschild, 1992; Lanyi, 1993; Grigorieff et al., 1996). Previous denaturation studies carried out by DSC and spectroscopic techniques have thrown light on the importance of several structural features on BR's stability, such as the presence of the retinal moiety, the favorable packing and interactions of the seven helices within the bilayer, the presence of cations in the medium, and the possible role of the extramembranous loops connecting the helices (Jackson & Sturtevant, 1978; Brouillette et al., 1987; Cladera et al., 1988, 1992a; Khan et al., 1992; Sanchez-Ruiz & Galisteo, 1993; Taneva et al., 1995). The question still remains, however, as to what extent these stability factors, and certain others proposed in the literature (Khan et al., 1992), are quantitatively comparable with each other, and whether they are interconnected to any degree or can be considered in principle as being simply additive factors.

We have made DSC and FTIR studies into the thermal stability of bacteriorhodopsin cleaved within different loops (individual peptide bonds 71–72 and 155–156, and both) at neutral and alkaline pH values and different scan rates and compared these results to those of the native protein. The denaturation of some of the samples followed the two-state kinetic model. When different BR molecule populations were present in the sample a clear cooperative intermolecular interaction appeared on denaturation. The

<sup>†</sup> This work was supported by DGICYT Grants PB93-1163 and PB92-0622 from the Ministerio de Educación y Ciencia (Spain), and 1995SGR00481 from the DGR (Generalitat de Catalunya). A.I.A. held a predoctoral fellowship from the Junta de Andalucía.

<sup>\*</sup> Author to whom correspondence should be addressed. Tel: +34-(9)58-243333/1. FAX: +34-(9)58-272879/274258.

<sup>‡</sup> Universidad de Granada.

<sup>§</sup> Universitat Autònoma de Barcelona.

<sup>®</sup> Abstract published in *Advance ACS Abstracts*, November 15, 1996.

<sup>1</sup> Abbreviations: DSC, differential scanning calorimetry; FTIR, Fourier-transform infrared spectroscopy; BR, bacteriorhodopsin; ABCDEFG, uncleaved bacteriorhodopsin; AB·CDEFG, chymotrypsin-cleaved bacteriorhodopsin in the 71–72 peptide bond; ABCDE·FG, NaBH-cleaved bacteriorhodopsin in the 155–156 peptide bond; AB·CDE·FG, double-cleaved bacteriorhodopsin in the 71–72 and 155–156 peptide bonds; FWHH, full width at half height;  $k$ , resolution enhancement factor.

effects of the cleavage of different peptide bonds on both  $T_m$  and  $\Delta H$  can be approximately taken as an additive result [see also Khan et al. (1992)]. FTIR studies always showed a moderate decrease in secondary-structure elements upon denaturation, which may be related to the lower denaturation  $\Delta H$  of this protein compared to that of globular proteins.

## MATERIALS AND METHODS

Purple membrane was obtained from *H. salinarium* strain S9 as described by Oesterhelt and Stoekenius (1974). Bleached membrane was obtained by the illumination of purple membrane suspensions ( $2.5 \times 10^{-5}$  M BR) with yellow light in the presence of 1 M hydroxylamine and 4 M NaCl at pH 7.5, as described by Oesterhelt et al. (1974). Purple membrane was regenerated by adding *all-trans*-retinal (1.4 mol of retinal/mol of BR) to an apomembrane suspension ( $10^{-5}$  M) in 50 mM phosphate buffer, pH 6.5. Retinal was dissolved in ethanol just before use, the concentration being determined using an extinction coefficient of  $42\,800\text{ M}^{-1}\text{ cm}^{-1}$  at 380 nm. The total ethanol concentration was less than 0.5% (v/v). After 24 h of incubation the sample was centrifuged at 2000g for 10 min to eliminate the excess of retinal.

Purple membrane (2 mg/mL in water) was cleaved by dilution with an equal volume of 6% (w/v)  $\text{NaBH}_4$  and 0.1 M sodium carbonate, pH 10. In order to obtain different percentages of cleaved BR, the samples were allowed to react at 4 °C in the dark for different periods under gentle stirring. The reaction was stopped by adding 5 volumes of 0.1 M phosphate buffer, pH 6. The sample was then washed three times with distilled water. Electrophoretic controls showed that after 4, 10, 24, and 48 h of reaction time 36%, 52%, 60%, and 86% of cleaved protein was obtained, respectively. For chymotryptic cleavage the apomembranes (2 mg/mL) were supplemented with Tris·HCl and  $\text{CaCl}_2$  (final concentrations 50 and 5 mM, respectively) and *N*-*p*-tosyl-L-lysine chloromethyl ketone (TLCK)-treated chymotrypsin (1 g/60 g BR), pH 8, and incubated for 3.5 h at 37 °C. Proteolysis was ended by cooling on ice and diluting at least one-to-one with ice-cold water containing a 1:3 mass ratio of chymotrypsin–trypsin (Bowman-Birk) inhibitor to the chymotrypsin present in the sample. After being pelleted, samples were resuspended in ice-cold water containing half as much inhibitor as before, and were pelleted again.

The protein concentrations for native bacteriorhodopsin and the modified, cleaved BR samples were determined from absorbance measurements at 568 nm using the absorption coefficient  $\epsilon = 63\,000\text{ M}^{-1}\text{ cm}^{-1}$  (Oesterhelt & Hess, 1973) and/or by Lowry's method (Lowry et al., 1951), modified according to Wang and Smith (1975). The molecular mass used was 26 kDa (Oesterhelt & Stoekenius, 1974). SDS–polyacrylamide gel electrophoresis was carried out using the discontinuous buffer system (Laemmli, 1970) with a 15% acrylamide separation gel. Gels were later stained with Procion Navy MXBRA (Sigma) and scanned with a Sharp JX-450 scanner. The areas of the resulting peaks were calculated with the PEAK program using native BR as the reference.

*all-trans* Retinal, trypsin–chymotrypsin inhibitor, and TLCK-treated chymotrypsin were from Sigma. All other chemicals were of the highest purity commercially available. Distilled, MilliQ deionized water was used throughout.

Calorimetric experiments were carried out in a DASM4 differential scanning microcalorimeter with 0.47 mL cells (Privalov & Potekhin, 1986). Prior to the DSC experiments the BR samples were extensively dialyzed against buffers with the appropriate pH. The scan rates used were 0.5, 1.0, and 2.0 K/min, and a constant pressure of 2 atm was always maintained to prevent possible degassing of the solutions on heating. Sample concentrations varied between 1.0 and 2.0 mg of protein/mL. DSC experiments were carried out at pH 7.5 (190 mM phosphate buffer) and at pH 9.5 (100 mM NaCl, 50 mM carbonate buffer) to follow the conditions used in a previous DSC work with BR (Galisteo & Sanchez-Ruiz, 1993). Reversibility of the transitions was checked for by reheating the solution in the DSC cell after cooling from the first run. Since the thermal transitions were always found to be irreversible, the reheating thermograms were used as instrumental base lines that were subtracted from the original, experimental thermograms to obtain the apparent  $C_p$  profiles. In addition, the thermograms were corrected for the dynamic response of the instrument (Lopez-Mayorga & Freire, 1987). The excess heat capacity function,  $C_p^{\text{ex}}$ , was obtained by drawing a chemical base line as described by Takahashi and Sturtevant (1981), which was subtracted from the apparent  $C_p$  curves. The existence in some cases of a pre-transition and/or an exothermic effect at high temperatures [also described by Brouillette et al. (1987) and Kahn et al. (1992), and which may be due to aggregation of denatured BR molecules] causes some uncertainty in the chemical base line, precluding the determination of  $\Delta C_p$  and increasing the errors (sometimes as large as  $\pm 30\%$ ) in the  $\Delta H$  values. Furthermore, since in most cases there were different populations in the samples, i.e., cleaved and uncleaved protein molecules and/or partially retinal-reconstituted BR molecules, the  $\Delta H$  values are only estimations of the real ones for the different species, a fact which does not, however, affect the qualitative conclusions of the work. The temperature at the  $C_p$  maximum,  $T_m$ , was determined to within 0.5 °C.

Membrane suspensions for the FTIR measurements were prepared by washing the membrane three times with  $\text{D}_2\text{O}$  buffer and keeping the final suspension overnight before data collection to achieve a good D/H exchange. Samples in  $\text{D}_2\text{O}$  (pD 6.0), at a protein concentration of about 20 mg/mL, were placed in 25 mm path length  $\text{CaF}_2$  IR cells with Teflon spacers. IR spectra were obtained on a Mattson Polaris FTIR spectrometer equipped with an MCT detector, working at an instrumental resolution of  $2\text{ cm}^{-1}$ . 1000 scans were averaged using a sample shuttle, apodized with a triangle function, and Fourier-transformed. The spectrometer was continuously purged with dry air (dew point lower than  $-40$  °C). To obtain the pure spectra of the membrane, spectra of the solvent were collected under identical conditions and digital subtractions were made by computer. The criterion for a good subtraction was the removal of the water band near  $2130\text{ cm}^{-1}$  and the obtention of a flat line between 1800 and  $2000\text{ cm}^{-1}$ . This region was also useful to check for the absence of residual water-vapor peaks. Deuterated buffers were prepared from a liophilized solution by adding  $\text{D}_2\text{O}$  and adjusting the measured pH (pH\*) with DCl. The pH\* value was corrected using the equation  $\text{pD} = \text{pH}^* + 0.4$  (Gregory & Rosenberg, 1986).

The experimental absorption spectra were Fourier-self-deconvoluted using the programs developed by Moffat et

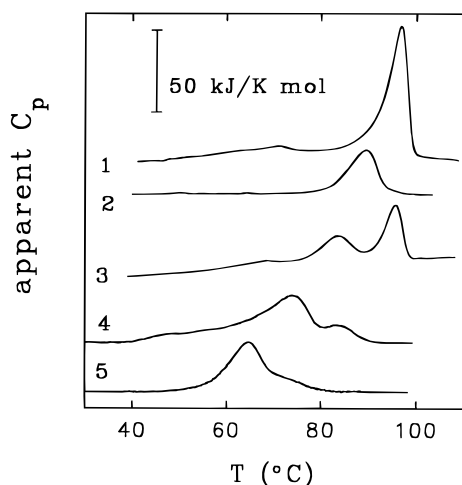


FIGURE 1: Original calorimetric recordings at 2 K/min of (1) native bacteriorhodopsin, pH 7.5; (2) chymotrypsin-cleaved bacteriorhodopsin, pH 7.5; (3) 52%  $\text{NaBH}_4$ -cleaved bacteriorhodopsin, pH 7.5; (4) chymotrypsin-cleaved and 86%  $\text{NaBH}_4$ -cleaved bacteriorhodopsin, pH 7.5; (5) chymotrypsin-cleaved and 86%  $\text{NaBH}_4$ -cleaved bacteriorhodopsin, pH 9.5.

al. (1986), with a Lorentzian band shape and FWHH and  $k$  values of  $14 \text{ cm}^{-1}$  and 2.5, respectively. In all cases the  $k$  values were kept below  $\log(\text{signal/noise})$ , as indicated by Mantsch et al. (1988). A least-square iterative curve fitting (Spectra Calc v2.21, from Galactic) was made over the deconvoluted spectrum using a Gaussian band shape and allowing the peak positions, heights, and bandwidths to vary simultaneously until a good fit was achieved.

## RESULTS

Figure 1 shows the DSC endotherms of native BR (ABCDEFG), chymotrypsin-cleaved BR at the 71–72 peptide bond within the loop between helices B and C (AB•CDEFG),  $\text{NaBH}_4$ -cleaved BR at the 155–156 peptide bond within the loop between helices E and F (ABCDE•FG), and double (chymotrypsin and  $\text{NaBH}_4$ ) cleaved BR (AB•CDE•FG). All samples cleaved with chymotrypsin were regenerated with *all-trans*-retinal after cleavage. The results for native BR compare well with others already published in the literature (Jackson & Sturtevant, 1978; Brouillette et al., 1987; Cladera et al., 1992a; Galisteo & Sanchez-Ruiz, 1993), i.e., a pre-transition at about 73 or 80 °C and the main denaturation transition, centered at about 81 or 95 °C, at pH 9.5 and 7.5, respectively. The AB•CDEFG sample shows a single transition endotherm at about 88–89 °C, pH 7.5, and 72–76 °C, pH 9.5, depending upon the scan rate, without any detectable pre-transition (Table 1); here the cleavage of the 71–72 peptide bond is practically 100%, so the single endotherm corresponds to the denaturation of the cleaved bacteriorhodopsin. Since the 155–156 peptide bond is only partially cleaved by  $\text{NaBH}_4$ , the two main DSC transitions in the endotherms of this modified BR should correspond to the denaturation of the two populations, ABCDEFG and ABCDE•FG present in the sample. The transition with the higher  $T_m$  corresponds in all probability to the denaturation of the uncleaved, native BR, whereas the lower  $T_m$  transition refers to the ABCDE•FG population. It is clear from Table 1 that the  $T_m$  value for this cleaved BR at pH 9.5, which falls within the range of 66–75 °C depending upon the scan rate, is also affected by the relative populations of both the native and cleaved BR

Table 1: Temperatures of the DSC Transitions for Several Bacteriorhodopsin Samples under Different Conditions<sup>a</sup>

sample	$\text{NaBH}_4$ cleavage (%)	pH	$\nu$ (K/min)	$T_1$ (°C)	$T_2$ (°C)
ABCDEFG	7.5	2.0	0.5	95.8	
			1.0	95.1	
			0.5	94.4	
	9.5	2.0	0.5	82.8	
			1.0	80.8	
			0.5	79.3	
AB•CDEFG	7.5	2.0	0.5	89.0	
			1.0	88.5	
			0.5	88.1	
	9.5	2.0	0.5	76.1	
			1.0	74.0	
			0.5	72.0	
ABCDE•FG	36	9.5	2.0	75.0	80.7
			1.0	73.0	78.6
			0.5	71.1	73.0
	52	9.5	2.0	73.3	77.9
			1.0	70.7	76.1
			0.5	69.8	75.8
	60	9.5	2.0	74.2	79.5
			1.0	69.8	75.8
			0.5	67.4	74.2
	86	9.5	2.0	71.5	
			1.0	68.9	
			0.5	66.5	
AB•CDE•FG	86	9.5	2.0	64.7	
			1.0	61.8	
			0.5	59.0	
	86	7.5	2.0	74.0	83.0
			1.0		
			0.5		

<sup>a</sup> The second column corresponds to the percentage of protein cleaved by  $\text{NaBH}_4$ . Cleavage by chymotrypsin was always about 100%.  $T_1$  and  $T_2$  are the  $T_m$  values for the different samples;  $T_1$  refers to cleaved bacteriorhodopsin, whereas  $T_2$  refers to the uncleaved protein, except for the last value of the  $T_2$  column, where it corresponds to partially cleaved protein (see text).

in the sample (see also Figure 4). This is also true for the  $T_m$  of the ABCDEFG fraction, which falls between 74 and 81 °C. The DSC pre-transition in these samples may well be due to the remaining native BR population. As for the AB•CDE•FG system, the sample has two BR-cleaved populations, the doubly cleaved BR and the one cleaved at the 71–72 bond alone. In fact the endotherms show two transitions, the main one at lower temperatures, 59–74 °C (Table 1), which would correspond to the AB•CDE•FG population, and a second one, which becomes a right-hand shoulder on the main transition at pH 9.5 (Figure 1), corresponding to the AB•CDEFG molecules. The smaller size of this second transition is due to the high extent of  $\text{NaBH}_4$  cleavage (86%) in our preparation.

As stated in Materials and Methods, the DSC transitions were always irreversible on a second heating of the samples, and we have also found that the denaturation temperature,  $T_m$ , of the endotherms was always clearly scan-rate dependent (Table 1). Galisteo and Sanchez-Ruiz (1993) have shown that the irreversible thermal denaturation of intact bacteriorhodopsin follows the two-state kinetic model (Sanchez-Ruiz et al., 1988) at pH 9.5, with an activation energy,  $E$ , of  $361 \pm 15 \text{ kJ/mol}$ . In our case, apart from native BR, the AB•CDEFG sample is the only one to show a single denaturation peak, corresponding to a single population of the cleaved protein. Therefore, we have used the DSC data of this sample at different scan rates to check whether they

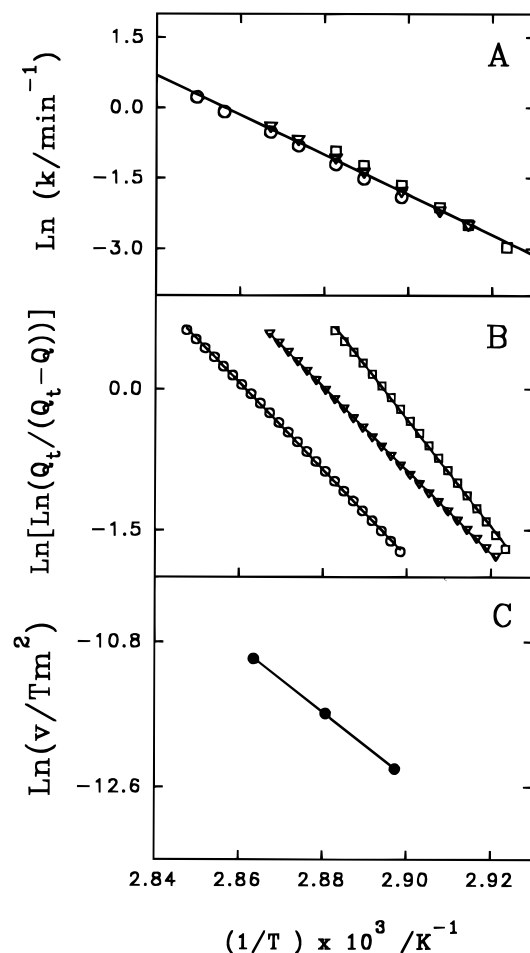


FIGURE 2: Two-state kinetic model plots for AB·CDEFG at pH 9.5. (A) Arrhenius plot: (○) 2 K/min, (▽) 1 K/min, (□) 0.5 K/min. (B) Plot of  $\ln[\ln(Q_t/(Q_t - Q))]$  versus  $1/T$ , where the symbols stand for the same as in (A). (C) Plot of  $\ln(v/T_m^2)$  versus  $1/T_m$ , where each data point refers to one of the three scan rates used.

conform to the simple two-state kinetic model. The development of this model,  $N \rightarrow D$ , where N stands for the native state and D for the irreversible denatured state, leads to the following equations (Sanchez-Ruiz et al., 1988; Conejero-Lara et al., 1991):

(A) The first-order rate constant,  $k$ , at a given temperature,  $T$ , is given by

$$k = \frac{v C_p^{\text{ex}}}{\Delta H - \Delta H(T)} \quad (1)$$

where  $v$  stands for the scan rate,  $\Delta H$  for the total enthalpy, and  $\Delta H(T)$  and  $C_p^{\text{ex}}$  for the enthalpy and excess heat capacity at the given temperature, respectively. Obviously  $k$  values obtained at different scan rates must lead to the same Arrhenius plot, as is indeed the case for AB·CDEFG at pH 9.5 (Figure 2A). The  $E$  value obtained in the Arrhenius fitting is  $373 \pm 34$  kJ/mol.

(B) The temperature dependence of the enthalpy function results in

$$\ln \left[ \ln \frac{\Delta H(T)}{\Delta H(T) - \Delta H} \right] = \frac{E}{R} \left[ \frac{1}{T_m} - \frac{1}{T} \right] \quad (2)$$

where a plot of the first term of the equation  $vs 1/T$  should give straight lines for each scan rate with a slope equal to

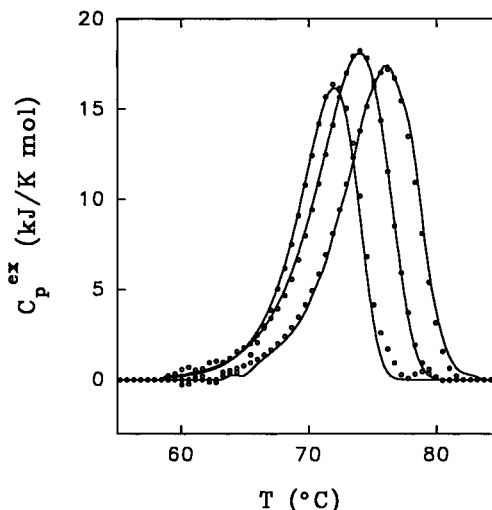


FIGURE 3: Temperature dependence of the  $C_p^{\text{ex}}$  for AB·CDEFG at pH 9.5 and three different scan rates (0.5, 1.0, and 2.0 K/min). Data points correspond to the experimental data and solid lines refer to the best nonlinear least-square fitting of eq 5.

$-E/R$ . This is shown in Figure 2B at pH 9.5 for the three scan rates used and the fittings lead to an average  $E$  value of  $392 \pm 60$  kJ/mol.

(C) The  $T_m$  value changes with the scan rate according to

$$\ln \left( \frac{v}{T_m^2} \right) = \text{const} - \frac{E}{RT_m} \quad (3)$$

The plot of  $\ln(v/T_m^2)$   $vs 1/T_m$  for the DSC data at pH 9.5 is in fact linear (Figure 2C), and the slope of the fit leads to an  $E$  value of  $336 \pm 13$  kJ/mol.

(D) The activation energy can also be calculated from the  $C_p^{\text{ex}}$  at the maximum of the DSC trace,  $C_p^{\text{m}}$ , according to

$$E = \frac{eRC_p^{\text{m}}T_m^2}{\Delta H} \quad (4)$$

The average  $E$  value at pH 9.5 obtained by this equation at the three scan rates is  $387 \pm 49$  kJ/mol.

(E) Finally, the shape of the DSC transitions that follow the two-state kinetic model is given by (Conejero-Lara et al., 1991)

$$C_p^{\text{ex}} = e \cdot C_p^{\text{m}} \exp \left( \frac{E\Delta T}{RT_m^2} \right) \exp \left[ -\exp \left( \frac{E\Delta T}{RT_m^2} \right) \right] \quad (5)$$

where  $\Delta T = T - T_m$ . The DSC transitions for AB·CDEFG at pH 9.5 are quantitatively described by this equation, as shown in Figure 3. The average  $E$  value obtained by a nonlinear least-square fitting of eq 5 to the experimental  $C_p^{\text{ex}}$  data at the three scan rates used is  $382 \pm 48$  kJ/mol.

Thus we may conclude that the thermal denaturation of the AB·CDEFG sample follows the two-state kinetic model with an overall average activation energy value of 374 kJ/mol, which compares very well with the  $E$  value for native BR at pH 9.5 (about 361 kJ/mol). On the other hand, the DSC data at pH 7.5 did not conform to the predictions of this simple kinetic model, as has also been shown to be the case with native BR at this same pH (Galisteo & Sanchez-Ruiz, 1993).

We have tried to analyze the two-peak endotherms of the sample containing both ABCDEFG and ABCDE·FG frac-

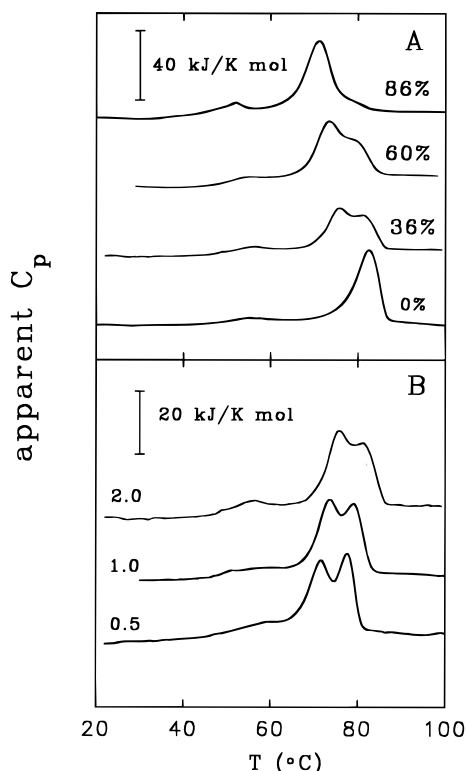


FIGURE 4: Apparent  $C_p$  profiles at pH 9.5 for: (A) different cleavage percentage (%) of ABCDE•FG at 2.0 K/min; (B) 36%-cleaved ABCDE•FG sample at three different scan rates (K/min).

tions (the  $\text{NaBH}_4$ -cleaved sample) at pH 9.5 by assuming that they conform to the sum of two two-state kinetic model transitions. To this end we carried out DSC experiments with samples containing different populations of both AB•CDEFG and ABCDE•FG at three scan rates (Figure 4). It is obvious that the high-temperature transition decreases concomitantly with cleavage and that the opposite is true for the low-temperature transition, both of which confirm that the former transition corresponds to the denaturation of the ABCDEFG population and the latter refers to that of the ABCDE•FG fraction. When we tried to analyze these DSC traces by deconvolution according to two sequential two-state transitions, however, we were unable to fit the overall calorimetric endotherms to the corresponding equations and obtain consistent values for the parameters involved at the different scan rates. This clearly suggests that the denaturation processes for both populations are not independent of each other. In fact the  $T_m$  of both transitions (Table 1 and Figure 4) decreases concomitantly with cleavage (i.e., the relative populations of both species), which can only be understood by assuming some kind of intermolecular interaction affecting the thermal stability of both ABCDEFG and ABCDE•FG.

As for the AB•CDE•FG sample (Figure 1 and Table 1), it is evident that its  $T_m$  is lower under all conditions than the  $T_m$  of both the AB•CDEFG and ABCDE•FG samples. Since the fraction of the AB•CDEFG molecules is quite low (14%) in this sample we could not estimate the  $T_m$  at pH 9.5, where the small transition becomes a right-hand shoulder on the main, low-temperature transition (Figure 1); at pH 7.5 and 2 K/min the  $T_m$  of the high-temperature transition, 83 °C, is lower than that of the pure AB•CDEFG sample under these conditions, 89 °C (Table 1). This comparison once again supports the existence of intermolecular interactions affecting

the thermal stability of different BR molecules present in the membrane.

The average  $\Delta H$  values for ABCDEFG obtained from the experiments at the three scan rates used (Table 1) are 354 and 417 kJ/mol at pH 7.5 and 9.5, respectively. These values compare well with those already published (Jackson & Sturtevant, 1978; Brouillette et al., 1987; Cladera et al., 1992a; Kahn et al., 1992; Galisteo & Sanchez-Ruiz, 1993). The absence of retinal precludes the DSC transition at pH 6.5 in pure water (Cladera et al., 1992a). Nevertheless, without retinal but in the presence of salts (buffer) at both alkaline and at neutral pH a DSC transition appears for both intact and cleaved BR, the enthalpy of which is  $30\% \pm 5\%$  of that of the corresponding reconstituted samples (Cladera et al., 1992a; Khan et al., 1992). Assuming this 30% enthalpy value for the non-regenerated BR, and bearing in mind that retinal reconstitution for our AB•CDEFG samples was about 60%, the average  $\Delta H$  values obtained in our DSC experiments would be about 290 and 87 kJ/mol for regenerated and retinal-free AB•CDEFG, respectively, at pH 7.5, whereas the corresponding  $\Delta H$  values would be about 259 and 78 kJ/mol at pH 9.5. The distribution of the DSC enthalpy values for the ABCDE•FG sample between the cleaved and non-cleaved BR populations is complex since it depends on the cleavage percentage, which affects both  $T_m$  values (see above and Table 1) and very probably their corresponding enthalpies. Assuming as an initial approximation that the molar enthalpies for both populations are independent of their relative fractions, the set of DSC conditions included in Table 1 leads to about 300 and 275 kJ/mol at pH 9.5 for the average  $\Delta H$  values of ABCDEFG and ABCDE•FG, respectively. Finally, we have both AB•CDE•FG (86%) and AB•CDEFG (14%) populations in the BR sample cleaved within both the BC and the EF loops. Without making any distinction between the different populations the  $\Delta H$  value at pH 9.5, as an average estimation, is about 130 kJ/mol.

The thermal denaturation processes of these BR samples were also followed by FTIR. Figure 5 shows the deconvoluted infrared spectra at 20 and 95 °C in  $\text{D}_2\text{O}$  buffer, pD 9.5, for AB•CDEFG (Figure 6A), 86% cleaved ABCDE•FG (Figure 6B) and AB•CDE•FG (Figure 6C). The spectra of the AB•CDEFG and ABCDE•FG samples at 20 °C are similar to those of the native membrane, with the two main  $\alpha$  helix bands at 1665 and 1657  $\text{cm}^{-1}$  (Cladera et al., 1992b). The AB•CDE•EF spectrum at 20 °C, however, resembles those obtained for the other two cleaved samples at higher temperatures (50–60 °C; results not shown), revealing a less compact structure in the former sample. Upon heating the sample to 95 °C a new band gradually appears at 1623  $\text{cm}^{-1}$  for the three forms, which indicates the formation of intermolecular  $\beta$  sheets (Cladera et al., 1992b; Cladera & Padrós, 1992; Jackson & Mantsch, 1992), whereas the main peaks at 1665 and 1657  $\text{cm}^{-1}$  are replaced by a band at 1653  $\text{cm}^{-1}$ , most probably due to a slightly different type of  $\alpha$  helix (Surewicz & Mantsch, 1988; Arrondo et al., 1993).

Figure 6 shows a deconvoluted spectrum in the amide I region, together with the best fitted bands, of the AB•CDE•FG sample, taken at 20 °C after being heated up to 95 °C. Great similarities exist between these and the spectrum and fitted bands of the heat denatured ABCDEFG at neutral pH (Cladera & Padrós, 1992). The relative area values found

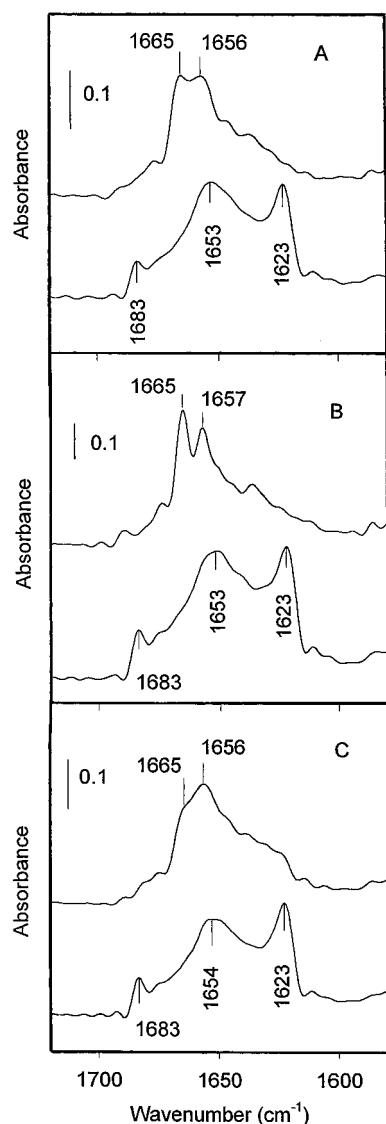


FIGURE 5: Deconvoluted Fourier-transform infrared spectra of membrane suspensions in D<sub>2</sub>O, pH 9.5. In each panel, the upper spectrum was taken at 20 °C and the lower one was taken at 95 °C. (A) AB·CDEF·G sample; (B) ABCDE·FG sample; (C) AB·CDE·FG sample. Deconvolutions were done using a FWHH of 14 cm<sup>-1</sup> and a *k* factor of 2.5.

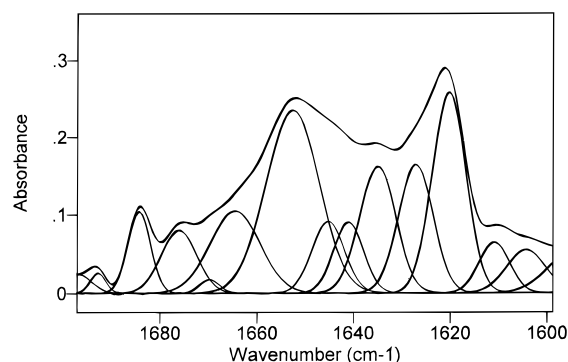


FIGURE 6: Deconvoluted Fourier-transform infrared spectrum of the sample AB·CDE·FG in D<sub>2</sub>O, pH 9.5, obtained at 20 °C after being heated to 95 °C, with the best-fit individual component bands.

here are as follows: reverse turns, 13% (bands at 1694, 1676, and 1664 cm<sup>-1</sup>);  $\beta$  sheets, 45% (bands at 1684, 1635, 1627, and 1620 cm<sup>-1</sup>);  $\alpha$  helices, 36% (bands at 1664, 1653, and 1641 cm<sup>-1</sup>), and unordered structures, 6% (band at 1645 cm<sup>-1</sup>). This secondary structure content after denaturation

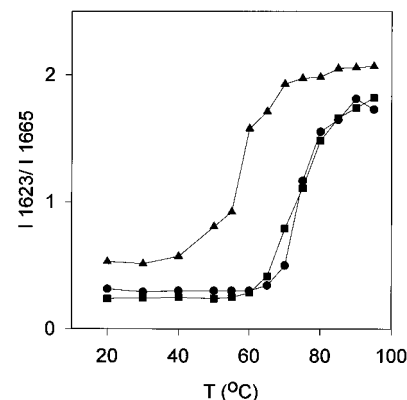


FIGURE 7: Ratio of intensities  $I_{1623}/I_{1665}$  measured from series of spectra of membrane suspensions in D<sub>2</sub>O, pH 9.5, taken at increasing temperatures. (●) AB·CDEF·G; (■) ABCDE·FG; (▲) AB·CDE·FG.

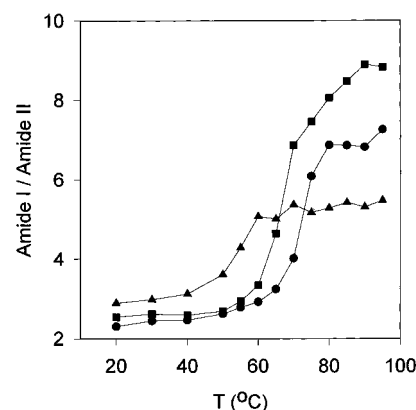


FIGURE 8: Ratio of areas amide I/amide II measured from the same spectra as in Figure 7, as a function of temperature. (●) AB·CDEF·G; (■) ABCDE·FG; (▲) AB·CDE·FG.

is again similar to that of the denatured ABCDEFG at pH 6.5 (Cladera & Padrós, 1992) and demonstrates the presence of significant amounts of  $\alpha$  helices in the denatured material.

Figure 7 shows the plots of the ratio of intensities at 1623 cm<sup>-1</sup> (indicative of  $\beta$  sheets) and 1665 cm<sup>-1</sup> (indicative of  $\alpha$  helices) for the three cleaved samples at pH 9.5. It is clear that the plots are compatible with the  $T_m$  values found by DSC, taking into account the different experimental conditions, particularly the heating rate and concentration. It is also evident in Figure 7 that AB·CDE·FG starts to denature at lower temperatures than the two samples with only one cleaved loop; for example, at about 60 °C half of the former sample population is already denatured, whereas both AB·CDEF·G and ABCDE·FG show only a small denatured fraction at this temperature. Figure 8 shows the ratio of the amide I/amide II areas, reflecting the percentage of H/D exchange. These plots lead to the same conclusions as those deriving from Figure 7. Thus, the conformational changes appearing upon temperature increase, which are responsible for the appearance of intermolecular  $\beta$  sheets, are paralleled by the increased accessibility of deuterons to the backbone protons of  $\alpha$  helices. The sigmoidal shape of the plots for the ABCDE·FG and AB·CDE·FG samples in both Figures 7 and 8 are slightly distorted at the right-hand side, probably due to the presence of NaBH<sub>4</sub>-uncleaved BR molecules with higher  $T_m$  values (see DSC Results).

## DISCUSSION

Some of the possible factors responsible for BR stabilization are the interactions of bound retinal with the protein and loops connecting the helices (Kahn et al., 1992). Furthermore we have demonstrated the importance of bound cations in the stability of BR in a previous study into the deionized and different cation-regenerated membranes (Cladera et al., 1988). Retinal does seem to play a major role in BR stability since the bleached or even the Schiff-base reduced proteins do not undergo the main DSC denaturation transition in water at pH 6.5 (Cladera et al., 1992a). Nevertheless, in the presence of salts at pH 7.5 bleached BR shows a small and wide DSC transition with a  $T_m$  at about 82 °C and a  $\Delta H$  value of about 110 kJ/mol, similar to that found for this sample at pH 7.0 ( $T_m = 85$  °C,  $\Delta H = 96$  kJ/mol) by Kahn et al. (1992).

Interhelical cooperativity in the denaturation process, as shown by a single DSC transition for AB•CDEFG (Figures 1 and 3), indicates that the cleaved helices unfold as a whole entity, as has previously been reported for this sample by Kahn et al. (1992). Our results for the two other cleaved BR samples, ABCDE•FG and AB•CDE•FG (see Results), lead to the same conclusion. Previous work (Cladera & Padrós, 1992; Cladera et al., 1992b; Taneva et al., 1995) has shown that the thermal denaturation of BR under different conditions leads to a compact denatured state, which retains a large proportion of ordered structure. Comparing the FTIR spectra of the denatured state of ABCDEFG (Cladera & Padrós, 1992) with that of AB•CDE•FG (Figure 6) it appears that both denatured states are similar in the overall content of secondary structure. Therefore, it would seem that loops do not contribute significantly to the final denatured BR state, but only serve to increase the thermal stability of the protein by holding the helices together.

The denaturation of the ABCDE•FG sample shows two DSC transitions (Figures 1 and 4), corresponding to the cleaved BR and to the ABCDEFG fraction also present in the sample (see Results). The  $T_m$  of both transitions depends, for a given scan rate, on the percentage of the two populations (Table 1), i.e., the thermal stability of each class of molecule is affected by the relative amount of the other class. Thus, the higher the ABCDEFG fraction the higher the  $T_m$  value for this molecule as well as for the ABCDE•FG molecule. This fact indicates that there must be intermolecular interactions between the different BR molecules leading to intermolecular cooperativity upon denaturation. Direct evidence for such cooperative behavior has been obtained here by studying mixtures with different populations of cleaved and uncleaved BR. Intermolecular BR contacts can be observed in the two-dimensional projections of purple membrane (Baldwin et al., 1988). As for the known DSC pre-transition observed in native BR, we show here that it would also seem to appear in the ABCDE•FG samples (Figures 1 and 4), where a fraction of the uncleaved protein is still present.

Under our experimental conditions the denaturation of all BR samples was irreversible, a fact already reported in the literature for some of these samples (Jackson & Sturtevant, 1978; Brouillette et al., 1987; Cladera et al., 1988, 1992a; Kahn et al., 1992; Taneva et al., 1995). In particular, uncleaved BR has been shown to undergo irreversible, scan-rate-dependent thermal denaturation at both pH 9.5 and 7.5

(Taneva et al., 1995), following, in the former case, the two-state kinetic model (Sanchez-Ruiz et al., 1988), with an activation energy of  $361 \pm 15$  kJ/mol (Galisteo & Sanchez-Ruiz, 1993). Our results with the ABCDEFG sample agree with those of Galisteo and Sanchez-Ruiz (1993) (results not shown). We also found that the denaturation of the other BR samples was highly scan-rate dependent (Table 1), i.e., that their thermal denaturation was a non-equilibrium, rate-limited process, thus taking place under kinetic control. This behavior is clear in our DSC results (Table 1 and Figures 3 and 4B) and therefore precludes any thermodynamic analysis of the DSC data. Since ABCDEFG follows the two-state kinetic model at pH 9.5, we have analyzed the data for the AB•CDEFG sample accordingly and have found that this cleaved BR also follows quantitatively the predictions of the model at pH 9.5 (Figures 2 and 3), with an average activation energy of 374 kJ/mol. This value practically coincides with that reported for intact BR, which means that the transition state and the denaturation pathway for both samples appears to be very similar. In addition, these activation energies are similar to the denaturation enthalpy for the two samples, which would seem to suggest that the conformation of the transition state would be similar to that of the final denatured state. On the other hand, and as expected from the DSC data analysis of native BR at pH 7.5, the AB•CDEFG sample did not follow the two-state kinetic model at pH 7.5.

Our attempts to fit the two transitions of the ABCDE•FG sample to a sum of two two-state irreversible transitions were unsuccessful, in the sense that the activation values for the two populations present in the sample, ABCDEFG and ABCDE•FG, disagreed with each other as far as the different percentages of cleaved BR are concerned. This result is in accord with the intermolecular interaction found for the denaturation of both species together, so their denaturation kinetics is somehow interconnected. This would lead to a much more complex kinetic behavior than the simple two-state model.

BR has been regenerated from its 1–71 and 72–248 fragments, where the complex is stabilized by the presence of retinal (Liao et al., 1983) and is functionally similar to the cleaved BR in purple membranes (Popot et al., 1987). Gilles-Gonzalez et al. (1991) have also shown that the loops between helices B and C and helices E and F can be shortened considerably without significant alteration to the BR function. The present and previous results give some indications as to the mechanism of BR thermal denaturation and to the contribution of retinal and the loops to BR stability. It is generally accepted that the presence of retinal bearing a protonated Schiff base induces a network of ionic and hydrogen bonding interactions which hold the helices together. Under these conditions a temperature increase gives rise to a cooperative transition at about 90 °C in water at pH 7. In the absence of retinal the network of interactions is still partially restored by salts, giving rise to a small DSC transition (Cladera et al., 1992a; Khan et al., 1992), whereas no DSC transition is apparent in pure water (Cladera et al., 1992a). It is as though the absence of retinal made the bundle looser, as recently shown by measuring the H/D exchange in the bleached sample compared to the native one (Cladera et al., 1996). When one or more loops are cleaved the network of interactions remains to some extent, although less thermal energy is then needed to open it. This is supported by the fact that when one or two loops are cleaved

H/D exchange starts to increase at lower temperatures than with native BR, especially in the case of the double-cleaved protein. The concept of helix separation on denaturation seems fully supported by the increase in H/D exchange, i.e., virtually the same  $T_m$  is seen by both DSC and FTIR (see Results), since a separation of the helices is necessary for deuterons to be able to enter into the interhelical space. This process is clearly cooperative, as shown by the sigmoidal shapes in Figure 8, where deuterons enter at lower temperatures when loops are cleaved.

The denaturation enthalpies for the AB•CDEFG sample fall within the range of 290–259 kJ/mol for the retinal-regenerated molecules and 87–78 kJ/mol for the retinal-free population, between pH 7.5 and 9.5 (see Results). These  $\Delta H$  values compare, within experimental uncertainty, with those reported for the individual bleached and reconstituted samples at pH 7 and 9 (Kahn et al., 1992). It is interesting to note that for this sample we obtain a single transition, which follows the two-state kinetic model despite both the bleached (40%) and reconstituted (60%) AB•CDEFG populations being present. It is difficult to rationalize the  $\Delta H$  estimations for the ABCDE•FG (275 kJ/mol) and AB•CDE•FG (130 kJ/mol) samples due to the assumptions made in obtaining these values (see Results). Nevertheless, it would seem that the cleavage within the B–C or E–F loops leads to very little change in  $\Delta H$ , whereas the decrease in  $\Delta H$  for the sample cleaved within both loops appears to be an additive effect, as has already been suggested by Kahn et al. (1992). This additive effect is also apparent in the thermal stability since the decrease in  $T_m$  observed for AB•CDE•FG (about 18 °C), is the sum of the about 7 and 11 °C observed for AB•CDEFG and ABCDE•FG, respectively, at pH 9.5 (Table 1).

Finally, according to both our present and earlier results (Cladera & Padrós, 1992; Cladera et al., 1992b), the low  $\Delta H$  for BR seems to be due to its limited partial disorganization, that is to say 20–30% of the secondary-structure elements on denaturation, e.g., from 62% to 45% in  $\alpha$  helices and from 16% to 13% in reverse turns. The latter, moderate decrease also shows, contrary to what could be expected, that the extramembrane portions do not appear to undergo extensive unfolding. The decrease in the above percentages for the denatured material agrees with the lower denaturation enthalpy of intrinsic membrane proteins, about 25–30%, as compared to that of water-soluble, globular proteins (Sanchez-Ruiz & Mateo, 1987).

## ACKNOWLEDGMENT

We thank Dr. J. Cladera for useful discussions, Dr. J. C. Martínez and Mrs. E. Serrano for technical help, and Dr. J. Trout for revising the English text.

## REFERENCES

- Arrondo, J. L. R., Muga, A., Castresana, J., & Goñi, F. (1993) *Prog. Biophys. Mol. Biol.* 59, 23–56.
- Baldwin, J. M., Henderson, R., Beckman, E., & Zemlin, F. (1988) *J. Mol. Biol.* 202, 585–591.
- Brouillette, C. G., Muccio, D. D., & Finney, T. K. (1987) *Biochemistry* 26, 7431–7438.
- Cladera, J., & Padrós, E. (1992) in *Structures and Functions of Retinal Proteins* (Rigaud, J. L., Ed.) Vol. 221, pp 33–36, John Libbey Eurotext Ltd., Montrouge, France.
- Cladera, J., Galisteo, M. L., Duñach, M., Mateo, P. L., & Padrós, E. (1988) *Biochim. Biophys. Acta* 943, 148–156.
- Cladera, J., Galisteo, M. L., Sabés, M., Mateo, P. L., & Padrós, E. (1992a) *Eur. J. Biochem.* 207, 581–585.
- Cladera, J., Sabés, M., & Padrós, E. (1992b) *Biochemistry* 31, 12363–12368.
- Cladera, J., Torres, J., & Padrós, E. (1996) *Biophys. J.* 70, 2882–2887.
- Conejero-Lara, F., Sanchez-Ruiz, J. M., Mateo, P. L., Burgos, F. J., Vendrell, J., & Avilés, F. X. (1991) *Eur. J. Biochem.* 200, 663–670.
- Galisteo, M. L., & Sanchez-Ruiz, J. M. (1993) *Eur. Biophys. J.* 22, 25–30.
- Gilles-Gonzalez, M., Engelman, D., & Khorana, H. (1991) *J. Biol. Chem.* 266, 8545–8550.
- Gregory, R. B., & Rosenberg, A. (1986) *Methods Enzymol.* 131, 448–484.
- Grigorieff, N., Ceska, T. A., Downing, K. H., Baldwin, J. M., & Henderson, R. (1996) *J. Mol. Biol.* 259, 393–421.
- Henderson, R., Baldwin, J. M., Ceska, T. A., Zemlin, F., Beckmann, E., & Downing, K. H. (1990) *J. Mol. Biol.* 213, 899–929.
- Jackson, M. B., & Sturtevant, J. M. (1978) *Biochemistry* 17, 911–915.
- Jackson, M., & Mantsch, H. H. (1992) *Biochim. Biophys. Acta* 1118, 139–143.
- Jackson, M., & Mantsch, H. H. (1995) *Crit. Rev. Biochem. Mol. Biol.* 30, 95–120.
- Kahn, T. W., Sturtevant, J. M., & Engelman, D. (1992) *Biochemistry* 31, 8829–8839.
- Klibanov, A. M., & Ahern, T. J. (1987) in *Protein Engineering* (Oxender, D. L., & Fox, C. F., Eds.) pp 213–218, Alan R. Liss, New York.
- Laemmli, U. K. (1970) *Nature* 227, 680–685.
- Lanyi, J. K. (1993) *Biochim. Biophys. Acta* 1183, 241–261.
- Liao, M.-J., London, E., & Khorana, H. (1983) *J. Biol. Chem.* 258, 9949–9955.
- Lopez-Mayorga, O., & Freire, E. (1987) *Biophys. Chem.* 87, 87–96.
- Lowry, O. H., Rosenbrough, N. J., Farr, A. L., & Randall, R. J. (1951) *J. Biol. Chem.* 193, 265–275.
- Mantsch, H. H., Moffatt, D. J., & Casal, H. (1988) *J. Mol. Struct.* 173, 285–298.
- Moffatt, D. J., Kauppinen, J. K., Cameron, D. G., Mantsch, H. H., & Jones, R. N. (1986) *NRCC Bulletin* 18, National Research Council of Canada, Ottawa, Canada.
- Oesterhelt, D., & Hess, B. (1973) *Eur. J. Biochem.* 37, 316–326.
- Oesterhelt, D., & Stoebenius, W. (1974) *Methods Enzymol.* 31, 667–678.
- Oesterhelt, D., Schuhmann, L., & Gruber, H. (1974) *FEBS Lett.* 44, 257–261.
- Popot, J. L., Gerchman, S., & Engelman, D. (1987) *J. Mol. Biol.* 198, 655–676.
- Privalov, P. L., & Potekhin, S. V. (1986) *Methods Enzymol.* 114, 4–51.
- Rothschild, K. (1992) *J. Bioenerg. Biomembr.* 24, 147–167.
- Ruiz-Sanz, J., Ruiz-Cabello, J., Cortijo, M., & Mateo, P. L. (1992) *Eur. Biophys. J.* 21, 169–178.
- Sanchez-Ruiz, J. M. (1992) *Biophys. J.* 61, 921–935.
- Sanchez-Ruiz, J. M., & Mateo, P. L. (1987) *Cell Biol. Rev.* 11, 15–45.
- Sanchez-Ruiz, J. M., & Galisteo, M. L. (1993) *Eur. Biophys. J.* 22, 25–30.
- Sanchez-Ruiz, J. M., Lopez-Lacomba, J. L., Cortijo, M., & Mateo, P. L. (1988) *Biochemistry* 27, 1648–1652.
- Surewicz, W. K., & Mantsch, H. H. (1988) *Biochim. Biophys. Acta* 952, 115–130.
- Surewicz, W. K., Mantsch, H. H., & Chapman, D. (1993) *Biochemistry* 32, 389–394.
- Takahashi, K., & Sturtevant, J. M. (1981) *Biochemistry* 20, 6185–6190.
- Taneva, S. G., Caaveiro, J. M. M., Muga, A., & Goñi, F. M. (1995) *FEBS Lett.* 367, 297–300.
- Wang, C. S., & Smith, R. L. (1975) *Anal. Biochem.* 163, 414–417.